

1 **Rapidly increasing sulfate concentration: a hidden promoter of eutrophication in**  
2 **shallow lakes**

3 Chuanqiao Zhou<sup>a,1</sup>, Yu Peng<sup>a,1</sup>, Li Chen<sup>a</sup>, Miaotong Yu<sup>a</sup>, Muchun Zhou<sup>b</sup>, Runze Xu<sup>a</sup>,  
4 Lanqing Zhang<sup>a</sup>, Siyuan Zhang<sup>c</sup>, Xiaoguang Xu<sup>a,\*</sup>, Limin Zhang<sup>a</sup>, Guoxiang Wang<sup>a</sup>

5 <sup>a</sup> School of Environment, Nanjing Normal University, Jiangsu Center for Collaborative  
6 Innovation in Geographical Information Resource Development and Application,  
7 Jiangsu Key Laboratory of Environmental Change and Ecological Construction,  
8 Nanjing 210023, China

9 <sup>b</sup> China Aerospace Science and Industry Nanjing Chenguang group, Nanjing 210022,  
10 China

11 <sup>c</sup> School of Energy and Environment, Southeast University, Nanjing 210096, China

12 *\*Corresponding author: 1, Wenyuan Road, Xianlin University District, Nanjing,*  
13 *210023, China*

14 *E-mail address: [xxg05504118@163.com](mailto:xxg05504118@163.com)*

15 <sup>1</sup> Both authors contributed equally

16 **Keywords:** Sulfate reduction; iron reduction; phosphorus release; eutrophication;  
17 sulfate reduction bacteria

18 **Abstract:**

19 Except for excessive nutrient input and climate warming, the rapidly rising SO<sub>4</sub><sup>2-</sup>  
20 concentration is considered as a crucial contributor to the eutrophication in shallow  
21 lakes, however, the driving process and mechanism are still far from clear. In this study,  
22 we constructed a series of microcosms with initial SO<sub>4</sub><sup>2-</sup> concentrations of 0, 30, 60, 90,

23 120 and 150 mg/L to simulate the rapidly  $\text{SO}_4^{2-}$  increase of Lake Taihu subjected to  
24 cyanobacteria blooms. Results showed that the sulfate reduction rate was stimulated by  
25 the increase of initial  $\text{SO}_4^{2-}$  concentrations and cyanobacteria-derived organic matter,  
26 with the maximal sulfate reduction rate of 39.68 mg/L·d in the treatment of 150 mg/L  
27  $\text{SO}_4^{2-}$  concentration. During the sulfate reduction, the produced maximal  $\Sigma\text{S}^{2-}$   
28 concentration in the overlying water and acid volatile sulfate (AVS) in the sediments  
29 were 3.15 mg/L and 11.11 mg/kg, respectively, and both of them were positively  
30 correlated with initial  $\text{SO}_4^{2-}$  concentrations ( $R^2=0.97$ ;  $R^2=0.92$ ). The increasing  
31 abundance of sulfate reduction bacteria (SRB) was also linearly correlated with initial  
32  $\text{SO}_4^{2-}$  concentrations ( $R^2=0.96$ ), ranging from  $6.65 \times 10^7$  to  $1.97 \times 10^8$  copies/g. However,  
33 the  $\text{Fe}^{2+}$  concentrations displayed a negative correlation with initial  $\text{SO}_4^{2-}$   
34 concentrations, and the final  $\text{Fe}^{2+}$  concentrations were 9.68, 7.07, 6.5, 5.57, 4.42 and  
35 3.46 mg/L, respectively. As a result, the released TP in the overlying water, to promote  
36 the eutrophication, was up to 1.4 mg/L in the treatment of 150 mg/L  $\text{SO}_4^{2-}$  concentration.  
37 Therefore, it is necessary to consider the effect of rapidly increasing  $\text{SO}_4^{2-}$   
38 concentrations on the release of endogenous phosphorus and the eutrophication in lakes.

### 39 **1.Introduction**

40 Nowadays, cyanobacteria bloom in eutrophic lakes has become one of the most  
41 serious problems in freshwater lakes all over the world (Iwayama et al., 2017; Ho et al.,  
42 2019). Phosphorus, as a necessary nutrient for biological growth, is considered to be  
43 one of the main limiting factors of lake eutrophication (Ni et al., 2020). In recent years,  
44 the input of exogenous phosphorus has been effectively controlled, while the release of

45 endogenous phosphorus is still an urgent problem in eutrophic lakes (Liu et al., 2018;  
46 Guo et al., 2020). The release of endogenous phosphorus is affected by many factors,  
47 such as wind and wave and the cyanobacteria decomposition (Xu et al., 2018; Zhao et  
48 al., 2019). There are many forms of phosphorus in freshwater lake sediments, including  
49 aluminum bound phosphorus (Al-P), iron bound phosphorus (Fe-P), etc. Among them,  
50 Fe-P, formed under the condition of high dissolved oxygen (DO), is the most active  
51 form of phosphorus in the sediments, which has a more obvious response to the change  
52 of DO (Zhang et al., 2020). The accumulation and decay of cyanobacteria in eutrophic  
53 lakes will change the physical and chemical environments of water body and form  
54 anaerobic reduction conditions (Yan et al., 2017). This will facilitate the reduction of  
55 iron oxides and lead to the desorption and release of Fe-P in sediments, resulting in the  
56 increase of endogenous phosphorus release (Zhao et al., 2019).

57 Iron reduction plays an important role in natural ecosystems. It has been reported  
58 that dissimilatory reduction of iron accounts for 22% of the total amount of organic  
59 matter anaerobic mineralization in offshore areas (Thamdrup et al., 2004). According  
60 to the classical theory, iron oxides or hydroxides can adsorb phosphorus in the water  
61 and form Fe-P precipitation (Gunnars et al., 1997). In freshwater lakes, the lack of Fe(III)  
62 content or the diagenesis of organic phosphorus may be the reason for the lack of  
63 phosphorus in the overlying water. Therefore, the formation of iron oxides on the  
64 surface of sediments is closely related to the phosphorus cycle process (Amirbahman  
65 et al., 2003; Chen et al., 2014). The interaction between iron and phosphorus is reflected  
66 in the effect of adsorption and desorption of Fe oxide on the P content in the overlying

67 water, since Fe-P is the main internal source of phosphorus (Wu et al., 2019). Iron  
68 oxides can be used as both the source and destination of phosphorus in lake ecosystems  
69 (Mort et al., 2010; Azam et al., 2014). In anaerobic reduction environments, iron  
70 reduction can significantly promote the resolution of Fe-P. The  $\text{Fe}^{2+}$  generated by the  
71 reaction can form FeS solid with soluble sulfide. In addition, free  $\text{Fe}^{3+}$  will combine  
72 with humus to form stable complex, which further prevents the co-precipitation process  
73 of phosphorus and iron oxides (Mort et al., 2010; Zhang et al., 2020). Therefore, iron  
74 reduction process driven by cyanobacteria decomposition affects the circulation of  
75 phosphorus in freshwater lakes.

76 Due to the  $\text{SO}_4^{2-}$  concentration in seawater reaching 28 mM, sulfate reduction  
77 process with the participation of sulfate reduction bacteria (SRB) has received  
78 considerable attention in the basic material cycle of marine biogeochemistry (Fike et  
79 al., 2015; Pan et al., 2020). In freshwater lakes, the  $\text{SO}_4^{2-}$  concentration is less than 800  
80  $\mu\text{M}$ , which is generally considered insufficient for continuous sulfate reduction (Hansel  
81 et al., 2015). However, in recent years, with the continuous input of exogenous sulfur,  
82 the  $\text{SO}_4^{2-}$  concentration in freshwater lakes increases significantly and the degree of the  
83 eutrophication and the  $\text{SO}_4^{2-}$  concentration show a positive correlation (Dierberg et al.,  
84 2011; Yu et al., 2013). For instance, the  $\text{SO}_4^{2-}$  concentration in Lake Taihu, one of the  
85 typical eutrophic lakes worldwide, has increased from 30 to 100 mg/L in the past 70  
86 years and it will continue to rise in the future (Yu et al., 2013; Zhou et al., 2022). The  
87 impact of sulfate reduction on the material cycle of lake ecosystems may be far beyond  
88 our knowledge (Baldwin et al., 2012; Yu et al., 2013). On the other hand, it has been

89 reported that sulfate reduction process is one of the important ways of anaerobic  
90 metabolism of organic matter in freshwater lakes, and  $\sum S^{2-}$  produced by sulfate  
91 reduction process can mediate the iron reduction process (Jorgensen et al., 2019; Zhang  
92 et al., 2020). SRB mainly uses  $SO_4^{2-}$  as the electron acceptor to complete anaerobic  
93 respiration, and the sulfur compounds produced by anaerobic metabolism are bound  
94 with iron and so on, which are fixed in the sediments and form AVS on the surface of  
95 sediments (Holmer et al., 2001; Chen et al., 2016). Therefore, with the input of  
96 exogenous sulfur, sulfate reduction process produced  $\sum S^{2-}$  will further promote iron  
97 reduction in freshwater lakes.

98 In freshwater lakes, iron cycle affects the process of phosphorus cycle, and sulfur  
99 cycle plays an important role in regulating iron cycle. Therefore, the cycle of iron, sulfur  
100 and phosphorus in freshwater lakes is inseparable (Wu et al., 2019; Zhao et al., 2019).  
101 Studies have shown that even when  $SO_4^{2-}$  content was as low as 20 mg/L, the anaerobic  
102 metabolism of organic substrates was still dominated by sulfate reduction. Therefore,  
103 sulfate reduction process plays an important role in the lacustrine biochemical cycle  
104 (Hansel et al., 2015). In the absence of cyanobacteria, sulfate reduction doesn't occur  
105 even if the  $SO_4^{2-}$  concentration is higher (Zhao et al., 2021). This is because the  
106 accumulation and decomposition of cyanobacteria not only change the environment of  
107 water body, but also release a large amount of organic matter, which provides the  
108 necessary conditions for the circulation of iron, sulfur and phosphorus (Yan et al., 2017;  
109 Melemdez-Pastor et al., 2019). Therefore, under the co-effect of the increase of  $SO_4^{2-}$   
110 and the cyanobacteria decomposition, the sulfate reduction process and the effect of

111 iron reduction process on endogenous phosphorus release from sediments need to be  
112 further studied.

113 In this study, a series of different initial concentrations of  $\text{SO}_4^{2-}$  were set according  
114 to the variation trend of  $\text{SO}_4^{2-}$  concentrations over the years and the possible rising trend  
115 of eutrophic Lake Taihu. The effects of increased  $\text{SO}_4^{2-}$  concentration and cyanobacteria  
116 bloom on sulfate reduction coupled with the microbial processes were investigated. The  
117 dynamic changes of  $\text{Fe}^{2+}$  and  $\text{Fe}^{3+}$  concentrations during iron reduction were studied in  
118 order to reveal the effect of sulfate reduction on iron reduction. *In addition, the dynamic*  
119 *changes of phosphorus in the overlying water and sediment were investigated. Finally,*  
120 *the coupled sulfate, iron and phosphorus cyclic processes affected by the increasing*  
121 *sulfate concentration and cyanobacteria bloom were also comprehensively analyzed for*  
122 *elucidating the phosphorus release dynamics to tracking the hidden promoter of*  
123 *cyanobacteria bloom in eutrophic lakes.* The findings may be benefit for evaluating the  
124 effect of sulfate reduction in freshwater lakes and its impact on the promotion of iron  
125 reduction and the release of endogenous phosphorus.

## 126 **2. Materials and methods**

### 127 *2.1 Sample collection and preparation*

128 Lake Taihu (31°24' 40" N, 120°1' 3" E), one of the largest eutrophic shallow lakes  
129 in China, with an average depth of 2.4 m and an area of 2340 m<sup>2</sup> (Mao et al., 2021).  
130 Samples of sediments and cyanobacteria were collected in July 2020. *Sediments from*  
131 *the west shoreline of the lake (31°24'45"N, 120°0'42"E) were collected using a gravity*  
132 *core sampler. Cyanobacteria was collected and concentrated by sieving water through*

133 a fine-mesh plankton (250 mesh). All the sediment and cyanobacteria samples were  
134 stored in an incubator with ice packs and delivered to the laboratory immediately. The  
135 sediment samples were blended thoroughly, homogenized, and sieved (100 mesh) to  
136 the polyethylene bag. The cyanobacteria samples were flushed and centrifuged at 1500  
137 r/min for 5 min by a CT15RT versatile refrigerated centrifuge (China) and freeze-dried  
138 by Biosafer-10A. Different gradient sulfate concentrations were prepared from  
139 the high purity water and Na<sub>2</sub>SO<sub>4</sub>.

## 140 2.2 Set-up of incubation microcosms

141 To simulate the dramatical SO<sub>4</sub><sup>2-</sup> increase and cyanobacteria blooms of eutrophic  
142 Lake Taihu, a series of microcosms were constructed in this study. According to the  
143 ratio of surface sediments and the average water depth and the cyanobacteria  
144 accumulation density of 2500 g/m<sup>2</sup> during the breakout of cyanobacteria blooms of  
145 Taihu Lake, 100 g of sediment, 200 ml of water and 0.11 g of cyanobacteria powder  
146 were added into each bottle (Zhang et al., 2020). Meanwhile, according to the change  
147 trend of SO<sub>4</sub><sup>2-</sup> concentrations in Taihu Lake over the years and the possibility of further  
148 increase in the future (Yu et al., 2013), the SO<sub>4</sub><sup>2-</sup> concentrations in six microcosm  
149 systems were configured as: 30, 60, 90, 120, 150 mg/L, and a control without SO<sub>4</sub><sup>2-</sup>,  
150 respectively. The microcosm system adopted anaerobic bottles (Φ75 mm, length 180  
151 mm, volume 500 ml) as the reaction device. There were three replicates in each SO<sub>4</sub><sup>2-</sup>  
152 concentration experimental group. Each group was sampled 17 times on 1, 2, 3, 4, 5, 6,  
153 7, 9, 11, 14, 18, 23, 28, 33, 38, 43 and 48 d. Totally, there were 306 anaerobic bottles,  
154 and all the anaerobic bottles were placed in a biochemical incubator at a temperature of

155 25 °C. The water, gas and soil samples were collected by destructive sampling, that is,  
156 at each sampling point, 18 anaerobic bottles were opened for testing, which ensured the  
157 anaerobic environment and air pressure for other bottles. A part of sediment was used  
158 for microbe determination and kept in a refrigerator at -80 °C, and the rest sediment and  
159 other samples were kept at 0-4 °C for less than 24 h before analysis.

### 160 2.3 Chemical analytical methods

161 All water column and pore-water samples were filtered through 0.45 µm Nylon  
162 filters prior. Dissolved total phosphorus (DTP) was determined by colorimetry after  
163 digestion with  $K_2S_2O_8+NaOH$ , and the ammonium molybdate and ascorbic acid were  
164 used as chromogenic agents (Ebina et al., 1983). Water DO, oxidation and reduction  
165 potential (ORP) were measured using calibrated probes (MP525, China) during  
166 destructive sampling. The  $SO_4^{2-}$  was detected using the turbidimetric method with the  
167 stabilizer of  $BaCl_2$  and gelatin (Tabatabai et al., 1974), and the  $\sum S^{2-}$  was detected by  
168 methylene blue (Cline et al., 1969). Acid volatile sulfate (AVS), the  $\sum S^{2-}$  combined  
169 with metal ions formed compounds in sediments, was determined by zinc cold diffusion  
170 method (Hsieh et al., 1997).  $Fe^{2+}$  and  $Fe^{3+}$  was determined by colorimetric (Phillips  
171 et al., 1987). The sediment total phosphorus (TP) was extracted and determined by  
172 colorimetry (Ruban et al., 2001).

### 173 2.4 Quantification of SRB in sediments

174 In order to confirm the changes of sediment SRB in the microcosms, RT-QPCR  
175 technologies were used to determine the cell copy numbers of MPA and SRB on 0,7  
176 and 38 d in the sediments.



177 The sediment samples were collected and frozen at -80 °C in an ultra-low  
178 temperature freezer. The E.Z.N.A. ®Soil DNA Kit (Omega Bio-Tek, Norcross, GA,  
179 USA) was used to extract the total genomic DNA from each soil sample according to  
180 the manufacturer's instructions. Nucleic acid quality and concentration were  
181 determined by 1% agarose gel electrophoresis and NanoDrop 2000 UV  
182 spectrophotometer (Thermo Scientific, USA), respectively.

183 SRB in sediments were quantified using the quantitative polymerase chain  
184 reaction (qPCR) method. The qPCR with primer sets targeting DSR1F+ (5'-  
185 ACSCACTGGAAGCACGGCGG-3') and DSR-R (5'-GTGGMRCCGTGCAKRTT  
186 GG-3') were used for the SRB in this study. The q-PCR experiments were performed  
187 on a ABI7300 q-PCR instrument (Applied Biosystems, USA) using ChamQ SYBR  
188 Color qPCR Master Mix as the signal dye. Each 20 µL reaction mixture contained 2 µL  
189 of the template DNA and 16.5 µL of ChamQ SYBR Color qPCR Master Mix. Standard  
190 curves for each gene were obtained by the tenfold serial dilution of standard plasmids  
191 containing the target functional gene. All operations were followed the MIQE  
192 guidelines.

### 193 *2.5 Statistical analysis*

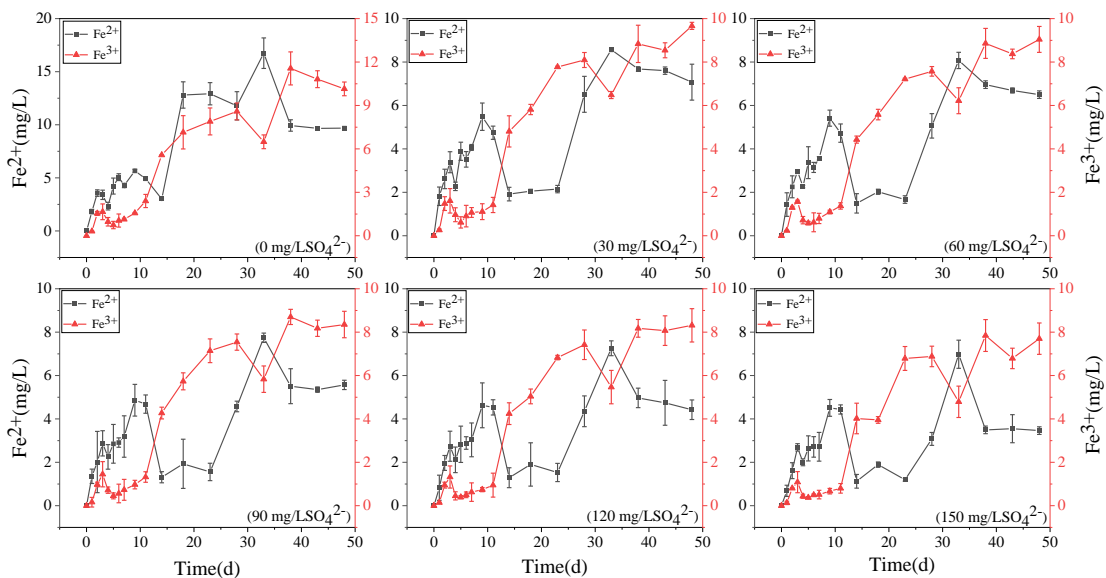
194 The Statistical Package of the Social Science 18.0 (SPSS 18.0) was used for  
195 statistical analysis. The one-way analysis of variance (ANOVA) and correlation  
196 analysis was carried out using bivariate correlations analysis.

197

## 198 **3.Results**

199 3.1  $Fe^{2+}$  and  $Fe^{3+}$  dynamics in overlying water

200 The concentration variations of  $Fe^{2+}$  and  $Fe^{3+}$  in overlying water during the  
201 incubation was presented in Fig.1. In the treatment without  $SO_4^{2-}$ , they increased  
202 continuously to 9.68 mg/L and 10.15 mg/L, respectively. The concentration of  $Fe^{3+}$  in  
203 the remaining five treatments decreased at the beginning and then increased to keep  
204 stable. The higher the initial sulfate concentration was, the lower the final  $Fe^{3+}$   
205 concentration displayed. In the initial 150 mg/L  $SO_4^{2-}$  concentration treatment, the final  
206  $Fe^{3+}$  concentration was the lowest of 7.7 mg/L. The  $Fe^{2+}$  concentration in the five  
207 treatments supplemented with  $SO_4^{2-}$  decreased significantly from 11 d to 23 d, and then  
208 increased to a stable level. The final concentration of  $Fe^{2+}$  also showed a negative  
209 correlation with the initial concentration of  $SO_4^{2-}$ . In the initial 30 mg/L  $SO_4^{2-}$   
210 concentration treatment, the final  $Fe^{2+}$  concentration was the highest of 7.07 mg/L.



211  
212 Figure 1. The concentration variations of  $Fe^{2+}$  and  $Fe^{3+}$  in the water column during the  
213 incubation

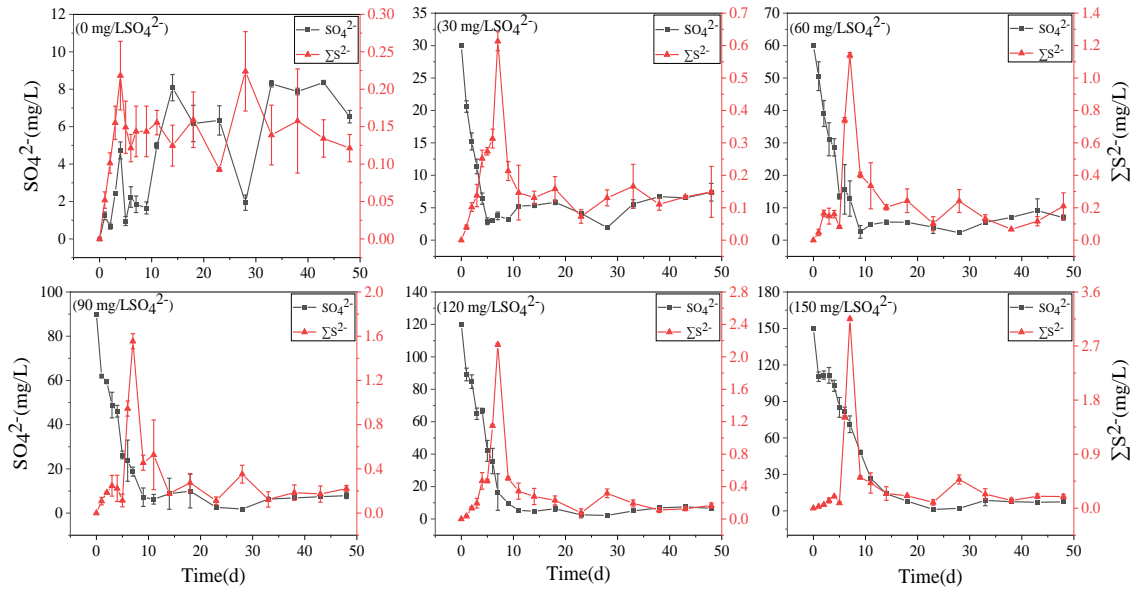
214 3.2  $SO_4^{2-}$  and  $\Sigma S^{2-}$  dynamics in overlying water

215 All treatments had obvious sulfate reduction reaction, and the concentration of  
 216  $\text{SO}_4^{2-}$  decreased greatly except for the treatment without adding  $\text{SO}_4^{2-}$  (Fig.2). The  
 217 higher the initial sulfate concentration was, the faster the sulfate reduction rate in the  
 218 initial stage exhibited (Tab.1). In the treatment with initial  $\text{SO}_4^{2-}$  concentration of 150  
 219 mg/L, the sulphate reduction rate was 39.68 mg/L·d, while it was only 9.39 mg/L·d in  
 220 the 30 mg/L  $\text{SO}_4^{2-}$  treatment. The sulfate reduction rate at the beginning of other  
 221 treatments was also positively correlated with the initial  $\text{SO}_4^{2-}$  concentration.

222 The higher the initial  $\text{SO}_4^{2-}$  concentration was, the higher the maximum  
 223 concentration of  $\sum\text{S}^{2-}$  was. In the treatment with initial  $\text{SO}_4^{2-}$  concentration of 30 mg/L,  
 224 the lowest concentration was 2.93 mg/L on the 5th day. However, the lowest  $\text{SO}_4^{2-}$   
 225 concentration appeared on the 23rd day was 1.18 mg/L in the treatment with initial  
 226  $\text{SO}_4^{2-}$  concentration of 150 mg/L. The maximum concentration of  $\sum\text{S}^{2-}$  was positively  
 227 correlated with the initial  $\text{SO}_4^{2-}$  concentration. In the initial  $\text{SO}_4^{2-}$  concentrations of 30,  
 228 60, 90, 120 and 150 mg/L  $\text{SO}_4^{2-}$  treatments, the highest  $\sum\text{S}^{2-}$  concentrations at 7 d were  
 229 0.14, 0.61, 1.14, 1.55, 2.15, and 3.15 mg/L, respectively.

230 Table 1. Sulphate reduction rate in the water column of microcosms (mg/L·d)

$\text{SO}_4^{2-}$ (mg/L) \ Time(d)	0	7	38
0	-	-	-
30	9.39	0.74	0.05
60	9.44	2.84	0.07
90	28.02	4.98	0.11
120	30.89	19.45	0.11
150	39.68	10.42	0.21



231

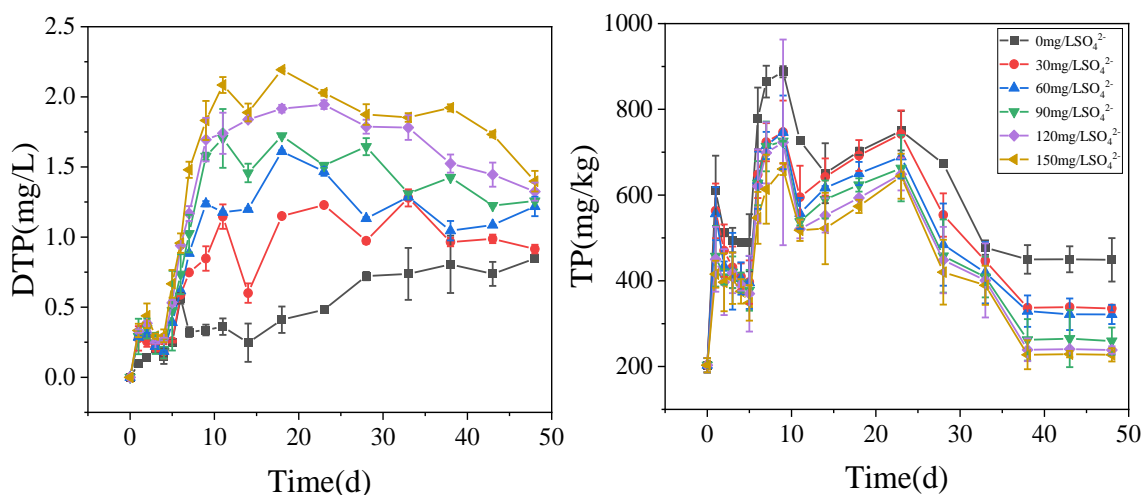
232 Figure 2. The concentration variations of  $\text{SO}_4^{2-}$  and  $\Sigma\text{S}^{2-}$  in the water column during  
 233 the incubation

### 234 3.3 TP dynamics in overlying water and sediments

235 The dynamics of DTP concentrations in overlying water during the incubation was  
 236 presented (Fig.3 left). The concentrations of DTP in overlying water were positively  
 237 correlated with the initial  $\text{SO}_4^{2-}$ . The higher the initial concentrations of  $\text{SO}_4^{2-}$  were, the  
 238 higher the concentrations of DTP in overlying water were. On 11 day, DTP in overlying  
 239 water continued to rise and then kept stable. The highest DTP concentration was 2.08  
 240 mg/L in the treatment with initial  $\text{SO}_4^{2-}$  concentration of 150 mg/L, while the highest  
 241 DTP concentration was 0.36 mg/L in the treatment without  $\text{SO}_4^{2-}$  addition.

242 The concentrations of TP in the sediments increased significantly in all treatments  
 243 with the cyanobacteria decomposition in the initial stage (Fig.3 right). Among of all  
 244 treatments, on 9<sup>th</sup> day, the highest concentration of TP in the sediments was 887.69  
 245 mg/kg in the treatment with initial  $\text{SO}_4^{2-}$  concentration of 0 mg/L. After 23 days, TP in  
 246 the sediments decreased significantly and then stabilized. During cyanobacteria

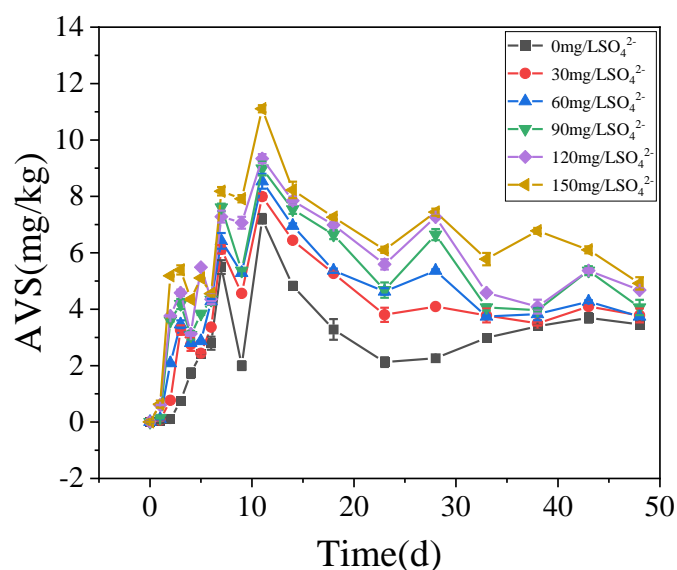
247 decomposition and sulfate reduction, the concentrations of TP in all treatments  
 248 negatively correlated with the initial  $\text{SO}_4^{2-}$  concentration. The final TP concentration  
 249 was 448.92, 335.32, 321.56, 259.32, 238.56 and 227.21 mg/kg, respectively in all  
 250 treatments.



251  
 252 Figure 3. The concentrations of TP in the overlying water (left) and sediments (right)  
 253 during the incubation

### 254 3.4 AVS dynamics in the sediments

255 The concentrations of AVS in the sediments were positively correlated with the  
 256 initial  $\text{SO}_4^{2-}$  concentrations. With the increase of TP in overlying water, the AVS in the  
 257 sediments also increased steadily and reached the peak on the 11st days. In the treatment  
 258 with initial  $\text{SO}_4^{2-}$  concentration of 0, 30, 60, 90, 120 and 150 mg/L, the highest  
 259 concentration of AVS in the sediments were 7.21, 7.99, 8.54, 8.99, 9.34 and 11.11  
 260 mg/kg, respectively.



261

262 Figure 4. The concentration of AVS in the sediments during the incubation

263 3.5 SRB dynamics in the sediments

264 During the decomposition of cyanobacteria, the SRB abundance significantly

265 increased compared with the initial stage ( $P < 0.01$ ). In the initial stage, the SRB

266 abundance was  $1.09 \times 10^8$  copies/g and the final value was positively correlated with the

267 initial  $\text{SO}_4^{2-}$ . On 7 d, SRB of all treatments showed a downward trend compared with

268 the initial value, and there was no significant difference in SRB values between each

269 treatment. On 38 d, except for the initial  $\text{SO}_4^{2-}$  concentrations of 0 and 30 mg/L, SRB

270 increased significantly in other treatments.

271 Table 2. Copy numbers of the *dsrB* gene of SRB in the sediments during the incubation

272 (copies/g)

Time $\text{SO}_4^{2-}$ (mg/L)	0 d	7 d	38 d
0	$1.09 \times 10^8$	$5.81 \times 10^7$	$6.65 \times 10^7$
30	$1.09 \times 10^8$	$6.13 \times 10^7$	$7.71 \times 10^7$
60	$1.09 \times 10^8$	$7.61 \times 10^7$	$1.15 \times 10^8$
90	$1.09 \times 10^8$	$7.87 \times 10^7$	$1.31 \times 10^8$
120	$1.09 \times 10^8$	$7.99 \times 10^7$	$1.49 \times 10^8$
150	$1.09 \times 10^8$	$8.23 \times 10^7$	$1.91 \times 10^8$

#### 273 4.Discussion

274 It is generally acknowledged that climate warming and exogenous nutrient input  
275 are the important contributors to the occurrence of cyanobacteria blooms (Anneville et  
276 al., 2015; Yan et al., 2017). However, in this study, we found that the dramatically  
277 increasing  $\text{SO}_4^{2-}$  concentration in eutrophic lakes is also a non-negligible promoter for  
278 the self-sustaining of cyanobacteria blooms. In eutrophic lakes, the decomposition of  
279 cyanobacteria consumed DO in the water, and formed strong anaerobic reduction  
280 conditions (Fig.S1). Fe-P was desorbed to from free  $\text{Fe}^{3+}$ , which was reduced to  $\text{Fe}^{2+}$  in  
281 anaerobic environments (Fig.1). Free  $\text{Fe}^{2+}$  combined with  $\sum\text{S}^{2-}$  which generated by  
282 sulfate reduction and eventually formed AVS fixed in the sediments (Fig.4), and  
283 phosphorus was released from the sediments (Fig.3). It has been reported that SRB and  
284 iron reduction bacteria (IRB) are the main microorganisms that drive sulfate reduction  
285 and iron reduction, respectively, and cyanobacteria decomposition promotes these  
286 microorganisms' growth (Wu et al., 2018). Consistent with these results, our findings  
287 also revealed that cyanobacteria released large amounts of organic matter to promote  
288 microbial growth during their decay and decomposition (Fig.S2, Tab. 2) and ultimately  
289 promoted anaerobic reduction of sulfur and iron (Holmer et al., 2001). Therefore, with  
290 increasing  $\text{SO}_4^{2-}$  concentrations in eutrophic lakes, the influence of sulfate reduction on  
291 phosphorus release is worth further investigation.

292 Sulfur and iron in eutrophic lake sediments are directly related to iron and  
293 phosphorus, and sulfur and phosphorus are also closely linked to bridges under the  
294 action of iron (Zhang et al., 2020). With the increase of  $\text{SO}_4^{2-}$  concentration in eutrophic

295 lakes, the effect of sulfate reduction on phosphorus release from sediments may be more  
296 important than previously recognized (Pester et al., 2012). Sulfate reduction driven by  
297 SRB is an important organic metabolism pathway in natural systems. During the sulfate  
298 reduction process,  $\text{SO}_4^{2-}$  is an electron acceptor and its concentration variation can  
299 significantly affect the sulfate reduction rate (Holmer et al., 2001; Nakagawa et al.,  
300 2012).  $\text{SO}_4^{2-}$  is reduced to  $\sum\text{S}^{2-}$  by acquiring the electrons supplied by SRB oxidation,  
301 and thus SRB plays an important role in sulfate reduction (Sela-Adler et al., 2017). The  
302 increase of  $\text{SO}_4^{2-}$  concentration promotes the SRB abundance, as evidenced by a  
303 positive correlation (Wu et al., 2018). In the case of increased SRB abundance (Tab. 2)  
304 and increased  $\text{SO}_4^{2-}$  concentration, the sulfate reduction reaction was enhanced. The  
305  $\text{SO}_4^{2-}$  concentration in the overlying water decreased significantly accompanied by a  
306 temporary increase in  $\sum\text{S}^{2-}$  (Fig.2). The highest concentrations of  $\sum\text{S}^{2-}$  also increased  
307 with the initial  $\text{SO}_4^{2-}$  concentrations (Fig.5a). Interestingly, the  $\sum\text{S}^{2-}$  decreased rapidly  
308 after day 10 to almost zero at the end (Fig.2). This may result from the two keys: (a)  
309 hydrogen sulfide overflows from the incubator; (b) sulfide migrates downward, and  
310 combines with other substances in the sediment and is immobilized (Zhang et al., 2020).  
311 In this study, TP in the overlying water has a significant positive correlation with the  
312 initial  $\text{SO}_4^{2-}$  concentrations ( $R^2 = 0.96$ ; Fig.3). The classical theory presumes that iron  
313 reduction by IRB leads to the release of iron-bound phosphorus in the anaerobic layer  
314 of sediments, and when the formed  $\text{Fe}^{2+}$  enters the aerobic water layer, it is oxidized by  
315  $\text{Fe}^{3+}$  and bound to phosphorus again (Roden et al., 2006; Chen et al., 2016). When the  
316 sulfate reduction process mediates the iron reduction process, the released  $\text{Fe}^{2+}$



317 combines with the product  $\sum S^{2-}$  of sulfate reduction to form Fe-S, thus weakening the  
318 reoxidation process of  $Fe^{2+}$ , and increasing the release of phosphorus (Mort et al., 2010;  
319 Zhao et al., 2019). Therefore, with the increase of  $SO_4^{2-}$  concentrations in eutrophic  
320 lakes, it significantly promoted the release of endogenous phosphorus from the  
321 sediments.

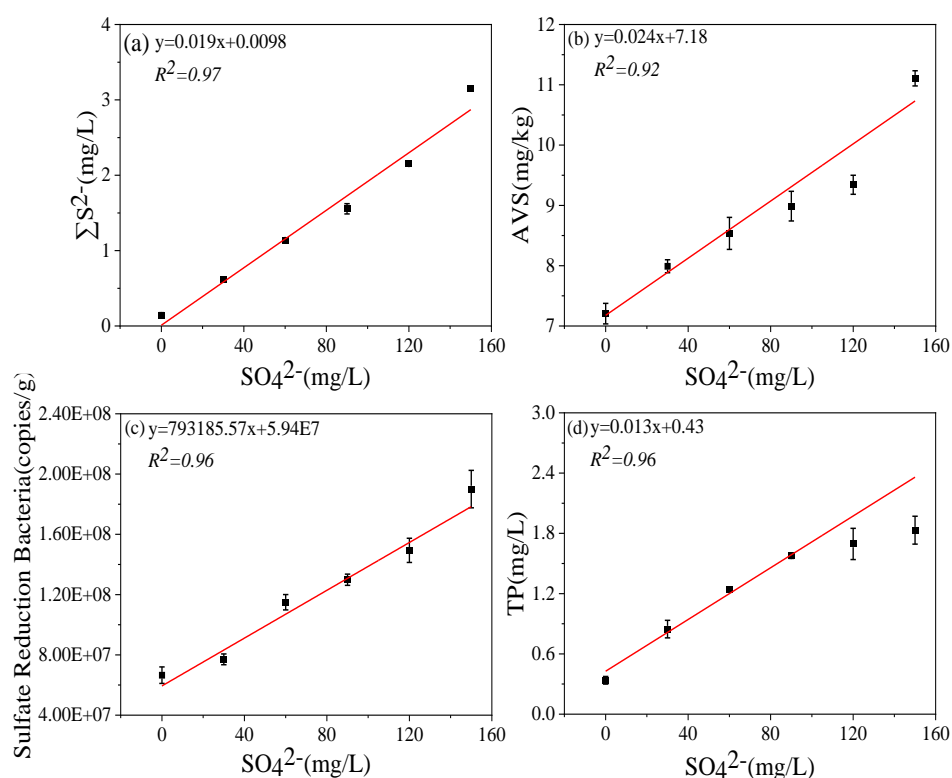
322 Although from a thermodynamic point of view, iron reduction should take  
323 precedence over sulfur reduction (Han et al., 2015). However, due to chemical kinetics,  
324 sulfur reduction occurs before iron reduction, resulting in the simultaneous appearance  
325 of  $\sum S^{2-}$  and iron oxides (Han et al., 2015; Hansel et al., 2015). This is consistent with  
326 the concentration variation of iron and sulfur in this study (Fig.1-3). It has been reported  
327 that iron cycles in the water body will produce an intense response to the accumulation  
328 of sulfide, that is, sulfate reduction can promote iron reduction (Friedrich et al., 2014;  
329 Zhang et al., 2020).  $\sum S^{2-}$  is the final product of sulfate reduction, which is toxic to  
330 microorganisms and easy to combine with heavy metals such as  $Fe^{2+}$  to form AVS in  
331 lake sediments (Holmer et al., 2001). In this study, the concentration of AVS showed a  
332 significant positive correlation with the initial concentration of  $SO_4^{2-}$  (Fig. 4, 5b), which  
333 was consistent with the highest concentration of  $\sum S^{2-}$  observed in the overlying water  
334 (Fig. 2, 5c). The concentrations of  $Fe^{2+}$  and  $Fe^{3+}$  in the overlying water increased  
335 significantly, and  $Fe^{2+}$  significantly decreased in the middle of the incubation (Fig. 1),  
336 suggesting that  $Fe^{2+}$  reduced by sulfate can be combined with the product  $\sum S^{2-}$  (Fig. 2).  
337 These results consistent with the trend that AVS in the sediments reached a peak after  
338 11 days and  $\sum S^{2-}$  in the water decreased rapidly after 9 days and remained at a lower

339 concentration (Fig. 2, 3). The reason for this phenomenon may be the formation of Fe-  
340 S compounds that is finally fixed in the sediments (Zhao et al., 2019).

341 The  $\Sigma S^{2-}$  mediated iron chemical reduction may lead to more environmental  
342 effects, such as phosphorus mobilization (Zhang et al., 2020). For instance, a previous  
343 investigation on [the lakes along the Yangtze River demonstrates that the effects of](#)  
344 [endogenous phosphorus release is probably related to the increase of  \$SO\_4^{2-}\$](#)   
345 [concentration \(Chen et al., 2016\)](#). In this study, the concentration of  $Fe^{2+}$  in the  
346 treatment without  $SO_4^{2-}$  continued to rise, and was up to the highest concentration  
347 among all treatments (Fig. 1). In contrast, the concentrations of TP in the treatment  
348 without  $SO_4^{2-}$  showed the lowest concentration among all treatments (Fig. 1, 5a). This  
349 is caused by  $Fe^{2+}$  and  $Fe^{3+}$  recombining with phosphorus and being immobilized in the  
350 sediments (Wu et al., 2019). In general, iron combines with phosphorus to form siderite  
351 ( $FePO_4 \cdot 2H_2O$ ) and blue iron ( $Fe_3(PO_4)_2 \cdot 8H_2O$ ) and is bound to the sediments (Taylor  
352 et al., 2011). However, when precipitation or reduction separates iron from iron  
353 phosphate minerals, phosphorus bound to iron is released (Gu et al., 2016).

354 In order to further elucidate whether the increasing  $SO_4^{2-}$  concentrations in  
355 overlying water result in the self-sustaining of eutrophication in shallow lakes, a  
356 conceptual diagram was put forward (Fig. 6). It has been accepted that exogenous  
357 nutrient inputs and climate warming have positive effects on the breakout of  
358 cyanobacteria blooms. With the continuous input of exogenous sulfur, the  $SO_4^{2-}$   
359 concentration in the lake water increases significantly. When cyanobacteria blooms  
360 start to decay, the overlying water shifts from the aerobic state to the strong anaerobic

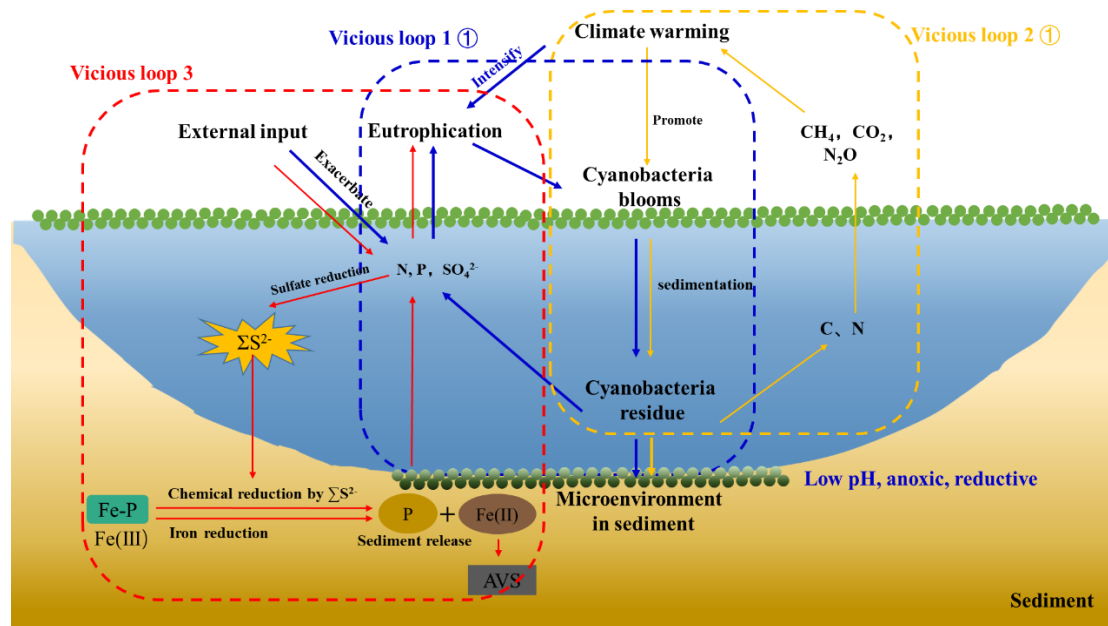
361 state, providing carbon source to promote the growth of microorganisms such as SRB.  
 362 The increasing  $\text{SO}_4^{2-}$  concentrations provide the electron for the sulfate reduction  
 363 process, resulting in the sulfate reduction and the release of a large amount of  $\Sigma\text{S}^{2-}$ . The  
 364  $\text{Fe}^{2+}$  released from the iron reduction process is captured by  $\Sigma\text{S}^{2-}$ , and finally the  
 365 combination of iron and P was reduced, promoting the release of endogenous  
 366 phosphorus. Therefore, it is necessary to pay attention to the effect of enhanced sulfate  
 367 reduction on endogenous phosphorus release in eutrophic lakes.



368

369 Figure 5. Correlation of initial  $\text{SO}_4^{2-}$  concentrations with  $\Sigma\text{S}^{2-}$  (a), AVS(b), Sulfate-  
 370 reducing bacteria (SRB) (c), TP (d) in the microcosm systems, respectively.

371



372

373 Figure 6. A simplified scheme of the relationship among climate warming, lake  
 374 eutrophication and cyanobacteria blooms in eutrophic lakes. Under climate warming  
 375 scenarios, extreme abiotic and biotic conditions facilitated the breakout of  
 376 cyanobacteria blooms. After their collapse, the high amount of N, P, and C were  
 377 released into the overlying water and reacted with the eutrophication. Furthermore, a  
 378 large amount of CH<sub>4</sub> and CO<sub>2</sub> was produced and emitted to the atmosphere, contributing  
 379 to global warming of freshwater lakes (Yan et al. 2017). With the external sulfur input,  
 380 the concentration of SO<sub>4</sub><sup>2-</sup> increased significantly and sulfate reduction was enhanced.  
 381 The cyanobacteria decomposition created an anaerobic reduction environment, which  
 382 will promote iron reduction and sulfate reduction. The free Fe<sup>3+</sup> generated by Fe-P  
 383 desorption was reduced to Fe<sup>2+</sup> and combined with ΣS<sup>2-</sup> which produced by sulfate  
 384 reduction to form stable Fe-S in the sediments. Phosphorus was released from the  
 385 sediment into the overlying water. Therefore, there are three vicious loops between  
 386 cyanobacteria blooms occurrence, lake eutrophication and climate warming.

387

388 **5.Conclusion**

389 The dramatical increase of  $\text{SO}_4^{2-}$  concentration was up to more than 100 mg/L in  
390 **eutrophic lakes**. There was a coupling relationship between sulfur, iron and phosphorus  
391 cycles in lake ecosystems. Rapidly increasing sulfate concentration enhanced the  
392 sulfate reduction to release of a large amount of  $\Sigma\text{S}^{2-}$  mediated by the increasing  
393 abundance of SRB with the adequate organic source from the decay processes of  
394 cyanobacteria blooms. The iron reduction, in positive with initial sulfate concentration,  
395 occurred with the cyanobacteria decomposition. The  $\text{Fe}^{2+}$  released from the iron  
396 reduction process was captured by  $\Sigma\text{S}^{2-}$ , and finally the combination of iron and P was  
397 reduced, promoting the release of endogenous phosphorus. Therefore, except for  
398 climate warming and excessive nutrients, the increasing sulfate concentration is proved  
399 to be another hidden promoter of eutrophication in shallow lakes.

400

401 **Author contributions**

402 Xu Xiaoguang: designed and led the study. Zhou Chuanqiao, Peng Yu, Chen Li,  
403 Yu Miaotong, Muchun Zhou, Xu Runze, Lanqing Zhang, Siyuan Zhang: performed the  
404 investigation and analysed the samples. Zhou Chuanqiao and Peng Yu: wrote the  
405 original draft with major edits and inputs from Xu Xiaoguang, Zhang Limin and Wang  
406 Guoxiang.

407

408 **Competing interests**

409 The authors declare that they have no known competing financial interests or

410 personal relationships that could have appeared to influence the work reported in this  
411 paper.

412

### 413 **Acknowledgements**

414 This work was supported by the National Natural Science Foundation of China  
415 (No.42077294, 41877336, 41971043), the Cooperation and Guidance Project of  
416 Prospering Inner Mongolia through Science and Technology (No.2021CG0037), the  
417 National Key Research and Development Program of China (No.2021YFC3200304),  
418 the Guangxi Key Research and Development Program of China (No.2018AB36010).

419

### 420 **References**

421 Amirbahman, A., Pearce, A.R., Bouchard, R.J., Norton, S.A., Kahl, J.S.: Relationship  
422 between hypolimnetic phosphorus and iron release from eleven lakes in Maine,  
423 USA, *Biogeochemistry*, 65(3), 369-385, 10.1023/A:1026245914721, 2003.

424 [Anneville, O., Domaizon, I., Kerimoglu, O., Rimet, F., Jacquet, S.: Blue-Green algae  
425 in a “Greenhouse Century”? new insights from field data on climate change impacts  
426 on cyanobacteria abundance, \*Ecosystems\*, 18\(3\), 441-458, 10.1007/s10021-014-  
427 9837-6, 2015.](#)

428 Azam, H.M., Finneran, K.T.: Fe(III) reduction-mediated phosphate removal as  
429 vivianite ( $\text{Fe}_3(\text{PO}_4)_2 \cdot 8\text{H}_2\text{O}$ ) in septic system wastewater, *Chemosphere*, 97, 1-9,  
430 100.1016/j.chemosphere.2013.09.032, 2014.

431 Baldwin, D.S., Mitchell, A.: Impact of sulfate pollution on anaerobic biogeochemical

432 cycles in a wetland sediment, *Water Research*, 46(4), 965-974,  
433 10.1016/j.watres.2011.11.065, 2012.

434 Chen, M., Li, X.H., He, Y.H., Song, N., Cai, H.Y., Wang, C.H., Li, Y.T., Chu, H.Y.,  
435 Krumholz, L.R., Jing, H.L.: Increasing sulfate concentrations result in higher  
436 sulfide production and phosphorous mobilization in a shallow eutrophic freshwater  
437 lake, *Water Research*, 96, 94-104, 10.1016/j.watres.2016.03.030, 2016.

438 Chen, M., Ye, T.R., Krumholz, L.R., Jiang H.L.: Temperature and cyanobacteria bloom  
439 biomass influence phosphorous cycling in eutrophic lake sediments, *Plos One*, 9(3),  
440 e93130, 10.1371/journal.pone.0093130, 2014.

441 Cline, J.D.: Spectrophotometric determination of hydrogen sulfide in natural waters,  
442 *Limnology and Oceanography*, 14, 454-458, 1969.

443 Dierberg, F.E., DeBusk, T.A., Larson, N.R., Kharbanda, M.D., Chan, N., Gabriel, M.C.:  
444 Effect of sulfate amendments on mineralization and phosphorus release from South  
445 Florida (USA) wetland soils under anaerobic conditions, *Soil Biology &*  
446 *Biochemistry*, 43(1), 31-45, 10.1013/j.soilbio.2010.09.006, 2011.

447 Ebina, J., Tsutsui, T., Shirai, T.: Simultaneous determination of total nitrogen and total  
448 phosphorus in water using peroxodisulfate oxidation, *Water Research*, 17(12),  
449 1721-1726, 1983.

450 Fike, D.A., Bradley, A.S., Rose, C.V.: Rethinking the ancient sulfur cycle, *Annual*  
451 *Review of Earth and Planetary Science*, 43, 593-622, 10.1146/annurev-warth-  
452 060313-054802, 2015.

453 Friedrich, M.W., Finster, K.W.: How sulfur beats iron, *Science*, 344(6187), 974-975,

454 10.1126/science.1255442, 2014.

455 Gu, S., Qian, Y.G., Jiao, Y., Li, Q.M., Pinay, G., Gruau, G.: An innovative approach  
456 for sequential extraction of phosphorus in sediments: Ferrous iron P as an  
457 independent P fraction, *Water Research*, 103, 352-361,  
458 10.1016/j.watres.2016.07.058, 2016.

459 Gunnars, A., Blomqvist, S.: Phosphate exchange across the sediment-water interface  
460 when shifting from anoxic to oxic conditions an experimental comparison of  
461 freshwater and brackish-marine systems, *Biogeochemistry*, 37(3), 203-226, 1997.

462 Guo, M.L., Li, X.L., Song, C.L., Liu, G.L., Zhou, Y.Y.: Photo-induced phosphate  
463 release during sediment resuspension in shallow lakes: A potential positive  
464 feedback mechanism of eutrophication, *Environmental Pollution*, 258, 113679,  
465 10.1016/j.envpol.2019.113679, 2020.

466 Han, C., Ding, S.M., Yao, L., Shen, Q.S., Zhu, C.G., Wang, Y., Xu, D.: Dynamics of  
467 phosphorus-iron-sulfur at the sediment-water interface influenced by algae blooms  
468 decomposition, *Journal of Hazardous Materials*, 300, 329-337,  
469 10.1016/j.jhazmat.2015.07.009, 2015.

470 Hansel, C.M., Lentini, C.J., Tang, Y.Z., Johnston, D.T., Wankel, S.D., Jardine, P.M.:  
471 Dominance of sulfur-fueled iron oxide reduction in low-sulfate freshwater  
472 sediments, *The ISME Journal*, 9(11), 2400-2412, 10.1038/ismej.2015.50, 2015.

473 Ho, J.C., Michalak, A.M., Pahlevan, N.: Widespread global increase in intense lake  
474 phytoplankton blooms since the 1980s, *Nature* 574, 667-670, 10.1038/s41589-019-  
475 1648-7, 2019.



476 Holmer, M., Storkholm, P.: Sulphate reduction and sulphur cycling in lake sediments:  
477 a review, *Freshwater Biology*, 46, 431-451, 10.1046/j.1365-2427.2001.00687.x,  
478 2001.

479 Hsieh, Y.P., Shieh, Y.N.: Analysis of reduced inorganic sulfur by diffusion methods:  
480 improved apparatus and evaluation for sulfur isotopic studies, *Chemical Geology*,  
481 137(3), 255-261, 1997.

482 Iwayama, A., Ogura, H., Hirama, Y., Chang, C.W., Hsieh, C.H., Kagami, M.:  
483 Phytoplankton species abundance in Lake Inba (Japan) from 1986 to 2016,  
484 *Ecological Research*, 32(6), 783-783, 10.1007/s11284-017-1482-z, 2017.

485 Jorgensen, B.B., Findlay, A.J., Pellerin, A.: The Biogeochemical sulfur cycle of Marine  
486 sediments, *Frontiers in Microbiology*, 10, 849, 10.3389/fmicb.2019.00849, 2019.

487 Liu, Z.S., Zhang, Y., Han, F., Yan, P., Liu, B.Y., Zhou, Q.H., Min, F.L., He, F., Wu,  
488 Z.B.: Investigation on the adsorption of phosphorus in all fractions from sediment  
489 by modified maifanite, *Scientific Reports*, 8, 15619, 10.1038/s41598-018-34144-w,  
490 2018.

491 Mao, Z.G., Gu, X.H., Cao, Y., Luo, J.H., Zeng, Q.F., Chen, H.H., Jeppesen, E.: How  
492 does fish functional diversity respond to environmental changes in two large  
493 shallow lakes? *Science of the total environment*, 753, 142158,  
494 10.1016/j.scitotenv.2020.142158, 2021.

495 Mort, H.P., Slomp, C.P., Gustafsson, B.G., Andersen, T.J.: Phosphorus recycling and  
496 burial in Baltic sea sediments with contrasting redox conditions, *Geochimica et*  
497 *Cosmochimica Acta*, 74(4), 1350-1362, 10.1016/j.gca.2009.11.016, 2010.

498 Melemdez-Pastor, I., Isenstein, E.M., Navarro-Pedreno, J., Park, M.H.: Spatial  
499 variability and temporal dynamics of cyanobacteria blooms and water quality  
500 parameters in Missisquoi Bay (Lake Champlain), *Water Supply*, 19(5), 1500-1506,  
501 10.2166/ws.2019.017, 2019.

502 Nakagawa, M., Ueno, Y., Hattori, S., Umemura, M., Yagi, A., Takai, K., Koba, K.,  
503 Sasaki, Y., Makabe, A., Yoshida, N.: Seasonal change in microbial sulfur cycling  
504 in monomictic Lake Fukami-ike, Japan, *Limnology and Oceanography*, 57(4), 974-  
505 988, 10.4319/lo.2012.57.4.0974, 2012.

506 Ni, Z.K., Wang, S.R., Wu, Y., Pu, J.: Response of phosphorus fractionation in lake  
507 sediments to anthropogenic activities in China, *Science of the Total Environment*,  
508 699, 134242, 10.1016/j.scitotenv.2019.134242, 2020.

509 Pan, P., Guo, Z.R., Cai, Y., Liu, H.T., Wang, B., Wu, J.Y.: High-resolution imaging of  
510 labile P&S in coastal sediment: Insight into the kinetics of P mobilization associated  
511 with sulfate reduction, *Marine Chemistry*, 225, 103851, 10.1016/j.marchem.2020.  
512 103851, 2020.

513 Pester, M., Knorr, K.H., Friedrich, M.W., Wagner, M., Loy, A.: Sulfate-reducing  
514 microorganisms in wetlands-fameless actors in carbon cycling and climate change,  
515 *Frontiers in Microbiology*, 3(72), 10.3389/fmicb.2012.00072, 2012.

516 Phillips, E.J.P., Lovley, D.R.: Determination of Fe(III) and Fe(II) in Oxalate Extracts  
517 of Sediment, *Soil Science Society of America Journal*, 51: 938-941, 1987.

518 Roden, E.E.: Geochemical and microbiological controls on dissimilatory iron reduction,  
519 *Comptes Rendus Geoscience*, 338(6-7), 456-467, 10.1016/j.crte.2006.04.009, 2006.

520 Ruban, V., Lopez-Sanchez, J.F., Pardo, P., Rauret, G., Muntau, H., Quevauviller, P.:  
521 Harmonized protocol and certified reference material for the determination of  
522 extractable contents of phosphorus in freshwater sediments-A synthesis of recent  
523 works, *Fresenius J Anal Chem*, 370, 224-228, 10.1007/s002160100753, 2001.

524 Sela-Adler, M., Ronen, Z., Herut, B., Antler, G., Vigderovich, H., Eckert, W., Sivan,  
525 O.: Co-existence of Methanogenesis and sulfate reduction with common substrates  
526 in sulfate-rich estuarine sediments, *Frontiers in Microbiology*, 8(766),  
527 10.3389/fmicb.2017.00766, 2017.

528 Tabatabai, M.: A rapid method for determination of sulfate in water samples,  
529 *Environmental*, 7, 237-243, 1974.

530 Taylor, K.G., Konhauser, K.O.: Iron in Earth surface systems: a major player in  
531 chemical and biological processes, *Elements*, 7(2), 83-87,  
532 10.2113/gselements.7.2.83, 2011.

533 Thamdrup, B., Dalsgaard, T., Jensen, M.M., Petersen, J.: Anammox and the marine N  
534 cycle, *Geochimica et cosmochimica acta*, 68(11), A325, 2004.

535 Wu, S.J., Zhao, Y.P., Chen, Y.Y., Dong, X.M., Wang, M.Y., Wang, G.X.: Sulfur  
536 cycling in freshwater sediments: A cryptic driving force of iron deposition and  
537 phosphorus mobilization, *Science of the total environment*, 657, 1294-1303,  
538 10.1016/j.scitotenv.2018.12.161, 2019.

539 Xu, G.H., Sun, Z.H., Fang, W.Y., Liu, J.J., Xu, X.B., Lv, C.X.: Release of phosphorus  
540 from sediments under wave-induced liquefaction, *Water Research*, 144, 503-511,  
541 10.1016 /j.watres.2018.07.038, 2018.

542 Yan, X.C., Xu, X.G., Wang, M.Y., Wang, G.X., Wu, S.J., Li, Z.C., Sun, H., Shi, A.,  
543 Yang, Y.H.: Climate warming and cyanobacteria blooms: Looks at their  
544 relationships from a new perspective, *Water Research*, 125, 449-457,  
545 10.1016/j.watres.2017.09.008, 2017.

546 Yu, T., Zhang, Y., Wu, F.C., Meng, W.: Six-Decade change in water chemistry of large  
547 freshwater lake Taihu, China, *Environmental Science and Technology*, 47(16),  
548 9093-9101, 10.1021/es401517h, 2013.

549 Zhang, S.Y., Zhao, Y.P., Zhou, C.Q., Duan, H.X., Wang, G.X.: Dynamic sulfur-iron  
550 cycle promoted phosphorus mobilization in sediments driven by the algae  
551 decomposition, *Ecotoxicology*, 30(8), 1662-1671, 10.1007/s10646-020-02316-y,  
552 2020.

553 Zhao, Y.P., Wu, S.J., Yu, M.T., Zhang, Z.Q., Wang, X., Zhang, S.Y., Wang, G.X.:  
554 Seasonal iron-sulfur interactions and the stimulated phosphorus mobilization in  
555 freshwater lake sediments, *Science of the total environment*, 768, 144336,  
556 10.1016/j.scitotenv.2020.144336, 2021.

557 Zhao, Y.P., Zhang, Z.Q., Wang, G.X., Li, X.J., Ma, J., Chen, S., Deng, H., Annalisa  
558 O.H.: High sulfide production induced by algae decomposition and its potential  
559 stimulation to phosphorus mobility in sediment, *Science of the total environment*,  
560 650, 163-172, 10.1016/j.scitotenv.2018.09.010, 2019.

561 Zhou, C.Q., Peng, Y., Deng, Y., Yu, M.T., Chen, L., Zhang, L.Q., Xu, X.G., Zhao, F.J.,  
562 Yan, Y., Wang, G.X.: Increasing sulfate concentration and sedimentary decaying  
563 cyanobacteria co-affect organic carbon mineralization in eutrophic lakes sediments,

564 Science of the total environment, 2022, 806, 151260, 10.1016/j.scitotenv.2021.  
565 151260, 2022.